

Generalized Contrastive Learning for Multi-Modal Retrieval and Ranking

Tianyu Zhu, Myong Chol Jung, and Jesse Clark

marqo ai, www.marqo.ai

{alan, david, jesse}@marqo.ai, tianyuzhu52@gmail.com

Abstract. Contrastive learning has gained widespread adoption for retrieval tasks due to its minimal requirement for manual annotations. However, popular contrastive frameworks typically learn from binary relevance, making them ineffective at incorporating direct fine-grained rankings. In this paper, we curate a large-scale dataset featuring detailed relevance scores for each query-document pair to facilitate future research and evaluation. Subsequently, we propose Generalized Contrastive Learning for Multi-Modal Retrieval and Ranking (GCL), which is designed to learn from fine-grained rankings beyond binary relevance score. Our results show that GCL achieves a **94.5%** increase in NDCG@10 for in-domain and **26.3** to **48.8%** increases for cold-start evaluations, measured **relative** to the CLIP baseline within our curated ranked dataset. Our dataset and code are available at: <https://github.com/marqo-ai/GCL>.

1 Introduction

Latent representations learnt via multi-modal contrastive methods have gained significant adoption for retrieval tasks within the research and vector database community [20, 21, 47, 48], largely because of their ease of access and minimal requirement for human annotations. However, despite its popularity, existing contrastive learning methods [8, 29, 33, 35] fail to incorporate nuanced ranking information, which is paramount for an effective information retrieval system. Furthermore, these methods typically employ a one-to-one mapping between queries and documents, overlooking the inherent many-to-many nature of search queries and results [9, 13, 30]. We believe the lack of research attention is primarily due to the absence of a public large-scale multi-modal retrieval dataset containing fine-grained ground-truth relevance scores [6, 16, 23, 26, 36, 37, 41, 45].

In this work, we collect a large-scale dataset comprising of around 10 million query and multimodal document pairs, each accompanied by fine-grained relevance score. We innovatively partition the dataset into in-domain, novel queries, novel documents and zero-shot sets, providing deeper insights for evaluations. The latter three are also referred to as cold-start evaluations. The dataset will be publicly available to accelerate research in learning to retrieve and rank. Leveraging this dataset, we introduce **Generalized Contrastive Learning for Multi-Modal Retrieval and Ranking (GCL)**, a training framework that integrates detailed relevance and ranking information. Unlike traditional contrastive learning

approaches [13, 29, 30] that rely on pairs of queries and documents with binary relevance, our framework generalizes this by incorporating a fine-grained weight for each pair, thus creating a triplet input unit. The weights are converted from ground-truth relevance score by a score-to-weight function. Weighted cross entropy loss is employed in our framework. GCL makes it possible to learn ranking based on historical data. For example, we can attribute a higher weight to a query-document pair if many people have downloaded the document after searching with this query. Moreover, GCL generalizes traditional single-field learning by training with multiple fields, merging elements such as title and product image into a weighted average embedding. This approach of utilizing simple mean embedding is consistent with practices in popular vector databases. We perform detailed ablation studies to demonstrate GCL’s effective integration of ranking and multi-field information. We also illustrate how the score-to-weight function can be customized to enhance various metrics. Relative to the baseline contrastive method [30], VITL14 trained with GCL shows a **94.5%** increase in NDCG@10 and a **504.3%** increase in ERR for in-domain evaluation. For cold-start evaluations, it exhibits relative improvements of **26.3 - 48.8%** in NDCG@10, **44.3 - 108.0%** in ERR, and **31.0 - 52.1%** in RBP. This large margin potentially unlocks numerous applications including vector search for ecommerce and retrieval-augmented generation.

In summary, our primary contributions are as follows: 1) We compile a large-scale multi-modal information retrieval dataset with fine-grained relevance scores; 2) We introduce an innovative split of the dataset that facilitates comprehensive evaluation insights; 3) We propose a novel contrastive learning framework that generalizes beyond binary relevance learning to accommodate fine-grained rankings; 4) We expand the conventional single-field representation of queries and documents to encompass multiple fields.

2 Related Works

2.1 Contrastive learning

Contrastive learning is a mechanism to map representations of similar instances (e.g., positive pairs) closer and dissimilar instances (e.g., negative pairs) further to each other. A seminal work of integrating contrastive learning in vision-language domain is CLIP [30] that maximizes cosine similarity of embeddings of image-text pairs through cross-entropy loss. Subsequent studies have extended the learning paradigm of CLIP [5, 13, 39, 47, 49]. The contrastive learning significantly improved a number of downstream tasks that include but are not limited to image classification [47, 48], object detection [40, 48], cross-modal retrieval [20, 21, 47, 48], image captioning [25, 47], and few-shot learning [51, 52].

In spite of the established efficacy of contrastive learning as a pre-training method, the vanilla contrastive learning methods are limited in their capacity to explicitly learn the rank order of documents given a query, thus constraining their utility in rank optimization. Additionally, these methods are constrained by their focus on maximizing similarity between individual instances (i.e., one-to-one

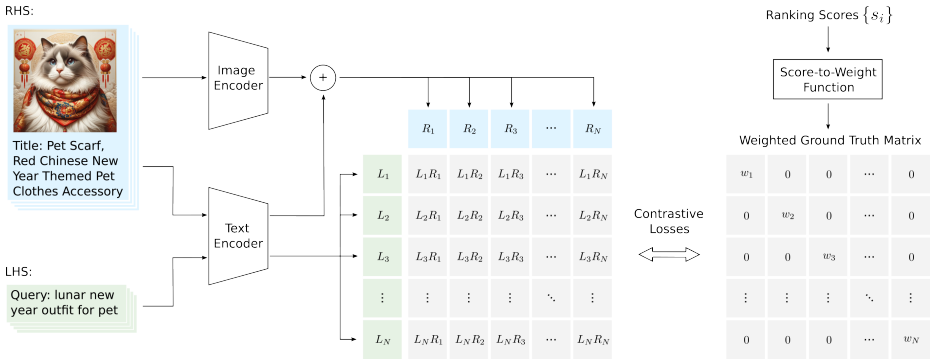


Fig. 1: Overview of our Generalized Contrastive Learning (GCL) approach. GCL integrates ranking information alongside multiple input fields for each sample (e.g., title and image) across both left-hand-side (LHS) and right-hand-side (RHS). Ground-truth ranking scores are transformed into weights, which are used for computing contrastive losses, ensuring that pairs with higher weights incur greater penalties.

similarity), thereby limiting the exploration of similarity relationships between sets of instances (i.e., many-to-many similarity). Our work aims to address these limitations, expanding the scope of contrastive learning to rank optimization and many-to-many similarity learning.

2.2 Information Retrieval Datasets

Information Retrieval (IR) datasets are designed to assess the retrieval and ranking capabilities of various models. However, comprehensive ranking information is notably lacking in most available datasets. While datasets like MSMARCO [26] excel in supporting tasks such as passage retrieval, question answering [16, 23, 45], biomedical retrieval [38], and fact checking [42], they predominantly provide binary (relevant/non-relevant) relevance score and focus a one-to-one query document relationship. Some datasets offer 3-5 levels of graded relevance [6, 36, 41], introducing gradations such as directly related, indirectly related, and non-related. However, these are typically limited to text-only formats and often only available for the test set. More critically, 3-5 levels are inadequate.

Another limitation of these datasets is their division into train, dev and test. Evaluating models solely on these development and test sets does not provide comprehensive insights into model performance across different scenarios, such as novel queries with existing documents, novel documents with existing queries, or completely zero-shot query-document pairs. This lack of diverse evaluation conditions hampers the ability to fully understand and measure the model’s adaptability and effectiveness in real-world information retrieval tasks. To overcome the limitations of existing datasets, we have acquired a multimodal dataset that features continuous (100 levels) relevance scores and many-to-many query-document relationships. This dataset is designed to provide a more granular understanding of model performance across various types of search scenarios.



Fig. 2: Visualization of the collected triplet dataset containing search queries (top row), documents and scores, showcasing thumbnails of returned products with scores that decrease linearly according to their positions. A noticeable contrast is observed between the image styles of fashion (left half) and home-related items (right half).

2.3 Neural information retrieval

Neural information retrieval (IR) aims to locate and retrieve relevant documents corresponding to queries by capturing semantic relationships between the queries and the documents learned from deep learning models [50]. Recent advancements of neural IR have been made in sparse retrieval methods to effectively reduce data dimensionality [10, 17], thereby enhancing retrieval efficiency via various methods such as term re-weighting [7, 22] and expansion methods [2, 12, 28, 44]. Similarly, significant advancements have been made in the domain of dense retrieval [15, 32, 46] by utilizing pre-trained language models like BERT [14, 27]. Despite the notable advancements achieved by these studies, the majority require a subsequent reranking stage after the initial retrieval. Our work takes a different approach by learning the retrieval and the ranking simultaneously, thereby introducing a unified single-stage retrieval system.

3 Approach

In this section, we first demonstrate the creation of a multi-modal information dataset that highlights the ranking problem in practical commercial scenario. We employ novel dataset splits to enhance evaluations. Following this, we describe our training framework GCL with the specialized loss functions taking triplets (query, document and weight) as input. Furthermore, we enable multi-field training for the embedding to absorb more document information.

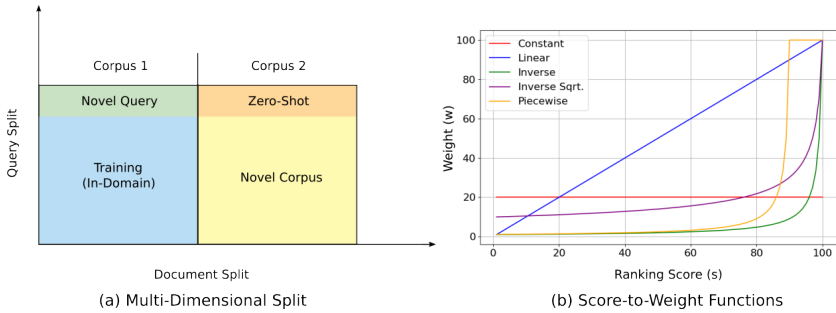


Fig. 3: (a) Illustration of multi-dimensional split along both query and document dimensions resulting in 4 splits: training split with 80% of queries and 50% of documents, novel query split with the other 20% of queries and the same documents as the training split, novel corpus split with the same queries as the training split and unseen documents with the equal size of the training corpus, and zero-shot split with unseen queries and documents. (b) Illustration of five distinct score-to-weight functions, designed to transform ground truth ranking scores into weights for the computation of losses.

3.1 Multimodal Information Retrieval Dataset with Rankings

Popular public datasets [26, 37, 42] for contrastive learning and information retrieval mostly focus on the one-to-one correspondence between the queries and documents. Those datasets that feature a one-to-many relationship are text-only and lack comprehensive document ranking [3, 34, 37]. These datasets do not encapsulate the ranking complexities present in real-world search scenarios, such as those found on e-commerce platforms. To investigate and tackle this problem, it is essential to obtain a multi modal dataset that focuses on the one-to-many query document relationship and includes rankings of the relevant documents. In this paper, We refer to this dataset as **GSPull-10M** which consists of **GSPullFashion-5M** and **GSPullHomeware-5M**. In this study, we chose to collect data via Google Shopping searches, as the returned product listings provide both images and texts, accompanied by meaningful rankings. In the remaining of this section, we show how we acquire the queries, documents and weights. Visualization of the dataset is in Figure 2.

Queries. For constructing a retrieval dataset through Google Shopping, achieving broad query coverage was critical. We focused on Fashion and Homeware as our main categories and identified 2.4k leaf categories using a taxonomy derived from Amazon. We then utilized GPT-4 [1] to craft 50 queries for each leaf category, ensuring a variety in word lengths. This process yielded around 120k queries, from which we randomly selected around 100k (98,236) for conducting searches on Google Shopping. We selected the Fashion category as it offers an excellent case study for multimodality, where both images and texts are crucial in conveying product information. The Homeware category was also chosen to facilitate a comparison, highlighting the unique aspects and challenges of multimodal information retrieval across different domains.

Algorithm 1 Single-Field GCL

- 1: **Input:** A batch of N triplets $(\mathbf{Q}, \mathbf{D}, \mathbf{w})$ of queries, documents and weights.
 - 2: Compute $\mathbf{Q}_f = E_q(\mathbf{Q})$ and $\mathbf{D}_f = E_d(\mathbf{D})$ with a query encoder E_q and a document encoder E_d .
 - 3: Normalize \mathbf{Q}_f and \mathbf{D}_f to unit vectors $\hat{\mathbf{Q}}_f$ and $\hat{\mathbf{D}}_f$.
 - 4: Compute dot product $\mathbf{Z} = \hat{\mathbf{Q}}_f \cdot \hat{\mathbf{D}}_f^T$.
 - 5: Compute loss $\mathcal{L} = \mathcal{L}_{WCE}(\mathbf{Z}, \mathbf{w})$ in Eq. (4).
 - 6: Back propagate \mathcal{L} to update E_q and E_d .
-

Documents. For our dataset, we utilize the Google Shopping API provided by SerpAPI to search for the queries. Each search yields 100 products. Same products can be returned by search different queries resulting a many-to-many mapping. The data for each product includes the title, a thumbnail link, and the product’s ranking position. We acquire the thumbnail image with wget tool.

Relevance/Ranking Scores. The ranking scores for GCL could be based on historic search logs where query-document pairs can be rated by their add-to-cart, click-through, or engagement rates. However, these metrics are often confidential and unavailable for public research. Consequently, we use the product ranking position from Google Shopping searches as a proxy. Google determines these rankings considering both the query and the product. To calculate the scores, we compute $s = 101 - rank$, so that it ranges from 1 to 100.

Multi Data Splits for Improved IR Evaluation. Referencing Section 2.2, conventional data splits (training, development, test) fail to precisely assess model performance on new queries, documents, or zero-shot scenarios. To address this, we adopt a multi-dimensional split strategy: splitting queries into an 80% training and 20% evaluation split, and splitting documents into two equal halves. This approach results in four sets: training, novel query, novel document, and zero-shot, with the latter comprising entirely unseen queries and documents. For evaluation, training and novel queries are tested against the first document corpus, while novel documents and zero-shot evaluations are conducted with the second corpus, ensuring a consistent corpus size across evaluations. The multi-split framework, depicted in Figure 3a, mirrors the varied challenges faced by real-world search systems, which encounter all four domains in differing volumes. In practical terms, evaluations conducted using the same data on which the model was trained are referred to as in-domain searches, while the other three evaluations represent various cold-start search scenarios. A weighted average of the results from these four evaluations, aligned with their respective traffic volumes, could offer a comprehensive benchmark for the system.

3.2 Incorporating Ranking Signals to Contrastive Learning

In this section, we present generalized contrastive learning (GCL), a novel framework that integrates ranking signals into the contrastive learning process by utilizing weights. Traditional contrastive learning techniques rely on a dataset comprising N_D pairs of (q_i, d_i) , where q_i and d_i denote the query and document for the i^{th} sample. In the context of the original CLIP framework [30], texts can

be considered as queries and images as corresponding documents. In contrast, our method employs a dataset consisting of N_D triplets of (q_i, d_i, w_i) , where w_i represents the weight. These weights are derived from desired relevance or ranking scores s_i by a Score-to-Weight function $w_i = STW(s_i) \in \mathbb{R}$. STW functions are used to shape the distribution of weights to help improving certain metrics. The higher score s_i of a document d_i , the greater its corresponding weight w_i will be. In our study, we have experimented with five different STW functions namely: constant, linear, inverse, inverse square root, and piecewise functions. Given a score s of an instance, the maximum of possible score s_{max} , and a constant c , the functions are defined as:

$$\text{Constant: } c, \quad \text{Linear: } s, \quad \text{Inverse: } \frac{s_{max}}{s_{max} - s + 1} \quad (1)$$

$$\text{Inverse square root: } \frac{s_{max}}{\sqrt{s_{max} - s + 1}} \quad (2)$$

$$\text{Piecewise: } \begin{cases} s_{max} & s \geq 0.9s_{max}, \\ \frac{s_{max}}{0.9s_{max} - s + 1} & s < 0.9s_{max} \end{cases} \quad (3)$$

When the constant function is used with $c = 1$, the weighted contrastive losses return to the original CLIP loss. The plot of the STW functions can be seen in Figure 3b.

For each training iteration, a batch of N triplets $(\mathbf{Q}, \mathbf{D}, \mathbf{w}) = (\{q_i\}_{i=1}^N, \{d_i\}_{i=1}^N, \{w_i\}_{i=1}^N)$ is randomly sampled. Query encoder E_q and document encoder E_d then encode the queries and documents into k -dimensional embeddings $\mathbf{Q}_f \in \mathbb{R}^{N \times k}$ and $\mathbf{D}_f \in \mathbb{R}^{N \times k}$ respectively. The embeddings are then normalized as $\hat{\mathbf{Q}}_f = \mathbf{Q}_f / \|\mathbf{Q}_f\|_2$ and $\hat{\mathbf{D}}_f = \mathbf{D}_f / \|\mathbf{D}_f\|_2$ where $\|\cdot\|_2$ is the l^2 -norm. The encoders can be text or image encoders depending on the data type of the queries and documents. The pairwise dot product results in $\mathbf{Z} = \hat{\mathbf{Q}}_f \cdot \hat{\mathbf{D}}_f^T \in \mathbb{R}^{N \times N}$, capturing the similarity scores between each query-document pair within the batch. The loss is computed from \mathbf{Z} and \mathbf{w} using weighted cross-entropy loss (see Section 3.3).

3.3 Weighted Contrastive Losses

Once the pairwise dot product matrix \mathbf{Z} is calculated, we apply a loss function designed to penalize low values on the diagonal and high values off the diagonal. The diagonal entries of \mathbf{Z} reflect the dot products of matching query-document pairs, indicating relevance. Off-diagonal entries, which represent dot products of non-matching pairs within the batch, serve as in-batch negatives. For CLIP and similar contrastive learning methods [13, 30, 47], the ground truth matrix is effectively an identity matrix, treating all diagonal values equally and neglecting the varying degrees of relevance between queries and documents. In our approach, we calculate this loss considering the weights \mathbf{w} , as depicted in Figure 1, to account for the relevance differences. We can treat the contrastive learning task as an n -class, n -sample classification problem, computing cross-entropy loss between the dot product matrix \mathbf{Z} and an identity matrix. Here, the i^{th} class corresponding

to the i^{th} sample is considered the ground truth. To infuse ranking information, our approach utilizes weighted cross-entropy loss,

$$\mathcal{L}_{WCE}(\mathbf{Z}, \mathbf{w}) = -\frac{1}{2N} \left(\sum_{i=1}^N w_i \log \left(\frac{\exp(\mathbf{Z}[i, i])}{\sum_{j=1}^N \exp(\mathbf{Z}[i, j])} \right) + \sum_{i=1}^N w_i \log \left(\frac{\exp(\mathbf{Z}[i, i])}{\sum_{j=1}^N \exp(\mathbf{Z}[j, i])} \right) \right) \quad (4)$$

where $\mathbf{Z}[i, j]$ denotes the element in the i^{th} row and the j^{th} column of \mathbf{Z} . This variation of cross-entropy loss assigns greater penalties to rows and columns with higher weights, biasing the gradients towards prioritizing their correction. This approach ensures that pairs deemed more relevant based on their weights are adjusted preferentially during the training process.

3.4 Generalized Contrastive learning with Multi-Field

Previous contrastive learning approaches [13, 13, 29, 30, 47] typically employ a single field to represent either a query or a document, even within multi-modal methodologies. For example, CLIP utilizes a single text field for the query and a single image field for the document. Our framework extends contrastive learning to a multi-field context, allowing both queries and documents to be represented by sequences of text and image fields. This approach mirrors real-world scenarios more closely, where a document often encompasses multiple fields such as a title, image, and description. To distinguish from the previous single field formulation, we now denote a batch of N triplets more generally as $(\mathbf{L}, \mathbf{R}, \mathbf{w}) = (\{\mathbf{L}^j\}_{j=1}^m, \{\mathbf{R}^j\}_{j=1}^n, \mathbf{w})$, which are left-hand-side fields (LHS), right-hand-side fields (RHS) and weights where m is the number of fields in LHS, n is the number of fields in RHS, \mathbf{L}^j denotes N samples of the j^{th} field in LHS, and \mathbf{R}^j denotes N samples of the j^{th} field in RHS.

During training, the data from each field are processed by their respective encoders E_j to extract embeddings as $\mathbf{L}^f = \{E_j(\mathbf{L}^j) \in \mathbb{R}^{N \times k}\}_{j=1}^m$ and $\mathbf{R}^f = \{E_j(\mathbf{R}^j) \in \mathbb{R}^{N \times k}\}_{j=1}^n$. Embeddings of each field are then normalized as done in Section 3.2 resulting in $\hat{\mathbf{L}}^f$ and $\hat{\mathbf{R}}^f$. Subsequently, a weighted average embedding is computed as $\hat{\mathbf{L}}_{avg}^f = \sum_{j=1}^m \gamma_{Lj} \times \hat{\mathbf{L}}_j^f$ and $\hat{\mathbf{R}}_{avg}^f = \sum_{j=1}^n \gamma_{Rj} \times \hat{\mathbf{R}}_j^f$ where $\gamma_L = \{\gamma_{Lj}\}_{j=1}^m$ and $\gamma_R = \{\gamma_{Rj}\}_{j=1}^n$ are the predetermined weights that sum to 1, and $\hat{\mathbf{L}}_j^f$ and $\hat{\mathbf{R}}_j^f$ represent the normalized embeddings of the j^{th} field. Finally, the dot product is computed by $\mathbf{Z}_{avg} = \hat{\mathbf{L}}_{avg}^f \cdot (\hat{\mathbf{R}}_{avg}^f)^T \in \mathbb{R}^{N \times N}$.

While the weighted mean embeddings of LHS and RHS serve to semantically represent the document, relying solely on the loss computed from dot product \mathbf{Z}_{avg} leads to significant performance degradation when searching with a single field query or when the document contains only text or image fields. This decline is attributed to the model being trained exclusively with mean weighted embeddings. To mitigate this issue, we compute pairwise dot products between each field on the LHS and each field on the RHS as $\{\{\mathbf{Z}_{jk}^{LR}\}_{j=1}^m\}_{k=1}^n$ where

Algorithm 2 Multi-Field GCL

- 1: **Input:** A batch of N triplets $(\mathbf{L}, \mathbf{R}, \mathbf{w})$, which are LHS fields, RHS fields, and weights. Hyperparameters γ_L and γ_R representing weights of each field. The number of fields in LHS as m and the number of fields in RHS as n .
 - 2: Compute $\mathbf{L}^f = \{E_j(\mathbf{L}^j)\}_{j=1}^m$ and $\mathbf{R}^f = \{E_j(\mathbf{R}^j)\}_{j=1}^n$ with a field-specific encoder E_j .
 - 3: Normalize embeddings of each field in \mathbf{L}^f and \mathbf{R}^f to obtain $\hat{\mathbf{L}}^f$ and $\hat{\mathbf{R}}^f$.
 - 4: Compute weighted average embeddings $\hat{\mathbf{L}}_{avg}^f = \sum_{j=1}^m \gamma_{L_j} \times \hat{\mathbf{L}}_j^f$ and $\hat{\mathbf{R}}_{avg}^f = \sum_{j=1}^n \gamma_{R_j} \times \hat{\mathbf{R}}_j^f$.
 - 5: Compute dot product between the averaged embeddings $\mathbf{Z}_{avg} = \hat{\mathbf{L}}_{avg}^f \cdot (\hat{\mathbf{R}}_{avg}^f)^T$.
 - 6: Compute dot product between each field of LHS and RHS
 $\{\{\mathbf{Z}_{jk}^{LR}\}_{j=1}^m\}_{k=1}^n = \{\{\hat{\mathbf{L}}_j^f \cdot (\hat{\mathbf{R}}_k^f)^T\}_{j=1}^m\}_{k=1}^n$.
 - 7: Compute loss $\mathcal{L} = \mathcal{L}_{WCE}(\mathbf{Z}_{avg}, \mathbf{w}) + \sum_{j=1}^m \sum_{k=1}^n \mathcal{L}_{WCE}(\mathbf{Z}_{jk}^{LR}, \mathbf{w})$.
 - 8: Back propagate \mathcal{L} to update all encoders.
-

$\mathbf{Z}_{jk}^{LR} = \hat{\mathbf{L}}_j^f \cdot (\hat{\mathbf{R}}_k^f)^T \in \mathbb{R}^{N \times N}$. Subsequently, we compute loss for training the multi-field generalized-CLIP:

$$\mathcal{L} = \mathcal{L}_{WCE}(\mathbf{Z}_{avg}, \mathbf{w}) + \sum_{j=1}^m \sum_{k=1}^n \mathcal{L}_{WCE}(\mathbf{Z}_{jk}^{LR}, \mathbf{w}). \quad (5)$$

While the loss can be computed with either \mathcal{L}_{WCE} or \mathcal{L}_{WSIG} , we used \mathcal{L}_{WCE} for this study. We leave the application of \mathcal{L}_{WSIG} as a future work. The overall algorithm is presented in Algorithm 2. Inspired by [49], we additionally experiment with weighted sigmoid loss. But it has not shown to work consistently, therefore we report them in the supplementary material.

4 Experiments

In this section, we evaluate the performance of GCL, contrasting its retrieval and ranking outcomes with the original CLIP [30] and other public contrastive learning methods using the curated Google Shopping dataset. Following this, we show detailed ablation studies focusing on score-to-weight functions, Multi-Field weight γ_{R_1} for documents, and variations in batch size. GCL is fine-tuned from pre-trained models sourced from OpenClip [5], using a learning rate of $1e-4$, consistent with the schedule reported in [5]. To ensure a robust evaluation of search systems, we sampled between 2500 and 5000 queries for both development and test sets across all four evaluation splits, resulting in eight distinct query sets for in-depth analysis. Except for batch size ablations, the development set is utilized for all ablation studies. Comparisons with publicly available methods, as described in Section 4.2, are conducted using the test set.

4.1 Evaluation Metrics

We use three main metrics to measure the retrieval and ranking performance.

Normalized Discounted Cumulative Gain (nDCG). nDCG [11] is one of the most widely used ranking measures for documents with graded relevance.

For a single query, it is defined as $nDCG = \frac{DCG}{IDCG}$ where $DCG = \sum_{i=1}^{n_{doc}} \frac{s_i}{\log_2(i+1)}$, n_{doc} is the number of documents for the query, and IDCG is the ideal DCG which is DCG with the ground-truth ranking order.

Expected Reciprocal Rank (ERR). ERR [4] is an extension of the traditional reciprocal rank metric to incorporate graded relevance. For a single query, it is defined as $ERR = \sum_{i=1}^{n_{doc}} \frac{1}{i} \prod_{j=1}^{i-1} (1 - R(s_j)) R(s_i)$ where $R(\cdot)$ is a mapping function from graded relevance to probability defined as $R(s_i) = \frac{s_i}{s_{max}+1}$, and s_{max} is the maximum relevance score for the query.

Rank Based Precision(RBP). RBP [24] is a retrieval metric that models users’ persistence of progressing from a document to the next document in a ranked list. For a single query, it is defined as $RBP = (1 - p) \sum_{i=1}^{n_{doc}} \frac{s_i}{s_{max}} p^{i-1}$ where p is a hyperparameter representing users’ persistence. In our experiments, we fixed p as 0.9, so that a user is expected looks at 10 items on average.

4.2 Comparison with Public Contrastive Learning Methods

This subsection presents a comparative analysis of the retrieval and ranking performance of GCL against established public contrastive learning frameworks. We conduct evaluations across four data splits: in-domain, novel queries, novel corpus, and zero-shot on GSFULL-10M dataset, utilizing metrics including NDCG@10, ERR, and RBP in Table 1. The evaluation considers text-based queries against three document formats: text-only (title), image-only, and multi-field (text and image). To maintain a fair comparison, all finetuned models listed in this table have been trained over 20 epochs with a batch size of 2048. In these studies, due to the generally low values of the metrics, often less than 0.1, we employ a relative measure, $\frac{b-a}{a} \times 100\%$, to illustrate the improvements of our methods compared to the baseline performances.

Text-To-Text Retrieval. In this study, we represent documents solely by product titles, thereby constructing a text-to-text retrieval scenario. We utilize the widely adopted BM25 [31] for initial comparisons. Our findings reveal that pre-trained text models, specifically E5 [43] and Roberta [31], surpass BM25’s performance. Further enhancements are observed when these models are fine-tuned on the GSFULL-10M dataset using their original frameworks. However, traditional frameworks lack the integration of explicit ranking information. In contrast, models fine-tuned using our GCL approach significantly outperform conventional methods in in-domain evaluations and exhibit marked improvements in cold-start scenarios. Numerically, our top-performing model, RobB, fine-tuned with GCL, has achieved a **32.8%** increase in NDCG@10 and a **308.1%** increase in ERR relative to RobB fine-tuned using the original method [19] for in-domain evaluation. For cold-start scenarios, it shows a **5.0 - 14.7%** improvement in NDCG@10 and a **38.9 - 92.3%** enhancement in ERR relative to Roberta [19].

Text-To-Image Retrieval. In this analysis, we represent documents solely by product thumbnail images, thereby constructing a text-to-image retrieval scenario. Results demonstrate that models fine-tuned with CLIP and SigLip on

Table 1: Retrieval and Ranking performance comparison of GCL versus publicly available contrastive learning methods [5, 18, 19, 31, 43, 49] assessed by NDCG@10, ERR, and RBP metrics on the GSFull-10M dataset. Encoders denoted with "*" have pre-trained weights from original sources and OpenClip [5, 43].

| | Methods | Encoders | In-Domain | | | Novel Queries | | | Novel Corpus | | | Zero-Shot | | |
|------------|-------------|--------------|--------------|--------------|--------------|---------------|--------------|--------------|--------------|--------------|--------------|--------------|--------------|--------------|
| | | | nDCG | ERR | RBP | nDCG | ERR | RBP | nDCG | ERR | RBP | nDCG | ERR | RBP |
| text-only | BM25 [31] | - | 0.071 | 0.028 | 0.052 | 0.067 | 0.026 | 0.049 | 0.071 | 0.024 | 0.053 | 0.068 | 0.026 | 0.050 |
| | E5 [43] | E5L* [43] | 0.150 | 0.061 | 0.118 | 0.147 | 0.058 | 0.116 | 0.147 | 0.059 | 0.117 | 0.150 | 0.063 | 0.116 |
| | E5 [43] | E5L [43] | 0.335 | 0.095 | 0.289 | 0.262 | 0.090 | 0.217 | 0.276 | 0.084 | 0.231 | 0.258 | 0.090 | 0.213 |
| | Cross E. | RobB* [19] | 0.102 | 0.033 | 0.077 | 0.106 | 0.038 | 0.078 | 0.104 | 0.030 | 0.077 | 0.105 | 0.035 | 0.078 |
| | Cross E. | RobB [19] | 0.332 | 0.099 | 0.288 | 0.272 | 0.091 | 0.225 | 0.280 | 0.090 | 0.236 | 0.263 | 0.088 | 0.217 |
| | GCL(ours) | E5L [43] | 0.431 | 0.400 | 0.347 | 0.299 | 0.172 | 0.244 | 0.286 | 0.119 | 0.239 | 0.271 | 0.116 | 0.223 |
| | GCL(ours) | RobB [19] | 0.441 | 0.404 | 0.355 | 0.312 | 0.175 | 0.253 | 0.294 | 0.125 | 0.245 | 0.279 | 0.128 | 0.229 |
| image-only | CLIP [30] | ViTB32* [30] | 0.063 | 0.025 | 0.052 | 0.063 | 0.024 | 0.052 | 0.061 | 0.020 | 0.051 | 0.063 | 0.024 | 0.052 |
| | CLIP [30] | ViTB32 [30] | 0.258 | 0.059 | 0.228 | 0.096 | 0.032 | 0.082 | 0.102 | 0.034 | 0.087 | 0.067 | 0.021 | 0.058 |
| | CLIP [30] | ViTL14* [30] | 0.081 | 0.031 | 0.067 | 0.077 | 0.027 | 0.063 | 0.079 | 0.029 | 0.065 | 0.079 | 0.026 | 0.065 |
| | CLIP [30] | ViTL14 [30] | 0.326 | 0.068 | 0.281 | 0.116 | 0.038 | 0.100 | 0.137 | 0.040 | 0.116 | 0.089 | 0.032 | 0.076 |
| | SigLip [49] | ViTB16 [30] | 0.168 | 0.042 | 0.139 | 0.087 | 0.030 | 0.072 | 0.092 | 0.029 | 0.076 | 0.070 | 0.023 | 0.058 |
| | GCL(ours) | ViTB16 [30] | 0.234 | 0.172 | 0.176 | 0.159 | 0.122 | 0.123 | 0.125 | 0.046 | 0.103 | 0.071 | 0.026 | 0.058 |
| | GCL(ours) | ViTB32 [30] | 0.449 | 0.564 | 0.329 | 0.141 | 0.124 | 0.111 | 0.101 | 0.040 | 0.086 | 0.074 | 0.032 | 0.062 |
| GCL(ours) | ViTL14 [30] | 0.489 | 0.530 | 0.362 | 0.160 | 0.124 | 0.127 | 0.125 | 0.047 | 0.104 | 0.091 | 0.036 | 0.078 | |
| multi | CLIP [30] | ViTL14 [30] | 0.310 | 0.093 | 0.252 | 0.205 | 0.075 | 0.165 | 0.228 | 0.081 | 0.184 | 0.199 | 0.079 | 0.159 |
| | GCL(ours) | ViTB32 [30] | 0.577 | 0.554 | 0.446 | 0.287 | 0.144 | 0.237 | 0.276 | 0.110 | 0.231 | 0.257 | 0.108 | 0.213 |
| | GCL(ours) | ViTL14 [30] | 0.603 | 0.562 | 0.467 | 0.305 | 0.156 | 0.251 | 0.288 | 0.118 | 0.241 | 0.272 | 0.114 | 0.224 |

the GSFull-10M dataset outperform their pre-trained counterparts. Yet, these conventional approaches do not incorporate specific ranking data. Conversely, our GCL framework, when applied for fine-tuning, markedly exceeds the performance of standard methods in in-domain assessments and shows substantial enhancements in cold-start conditions. Numerically, our best-performing model, ViTL14, fine-tuned with GCL, realized a **50.0%** increase in NDCG@10 and a **690.4%** increase in ERR relative to ViTL14 fine-tuned using the original CLIP method [30] for in-domain assessments. For cold-start situations, it exhibited an enhancement of **12.5%** - **226.3%** in ERR relative to CLIP. The exception occurs in the NDCG@10 metric for novel corpus evaluations, where GCL slightly underperforms compared to CLIP. Nonetheless, GCL exceeds CLIP in NDCG@10 by relatively **37.9%** and **2.2%** in Novel Queries and Zero-Shot.

Multi-Field Retrieval. The multi-field implementation of our GCL framework, which represents documents using both product images and titles, has significantly outperformed text-only and image-only counterparts, delivering the best overall results. The optimal configurations identified in the ablation studies (see subsection 3.4) were applied. While the original CLIP [30] also shows enhanced performance, it does not employ multi-field training. GCL’s integration of multi-field data and ranking signals has led to a remarkable **94.5%** increase in NDCG@10 and a **504.3%** increase in ERR relative to ViTL14 fine-tuned with the original CLIP method. In cold-start scenarios, GCL has shown superior performance to CLIP [30], with improvements of **26.3%** - **48.8%** in NDCG@10, **44.3%** - **108.0%** in ERR, and **31.0%** - **52.1%** in RBP.

Table 2: Comparing performance of GCL with various Score-to-weight functions using GSFashion-5M dataset and ViTB32 [30].

| STW | In-Domain | | | Novel Queries | | | Novel Corpus | | | Zero-Shot | | |
|---------------|--------------|--------------|--------------|---------------|--------------|--------------|--------------|--------------|--------------|--------------|--------------|--------------|
| | nDCG | ERR | RBP | nDCG | ERR | RBP | nDCG | ERR | RBP | nDCG | ERR | RBP |
| Constant | 0.419 | 0.088 | 0.367 | 0.197 | 0.065 | 0.164 | 0.192 | 0.060 | 0.162 | 0.194 | 0.063 | 0.158 |
| Linear | 0.583 | 0.163 | 0.483 | 0.217 | 0.084 | 0.180 | 0.197 | 0.066 | 0.167 | 0.201 | 0.073 | 0.163 |
| Inverse | 0.599 | 0.608 | 0.459 | 0.236 | 0.141 | 0.190 | 0.197 | 0.084 | 0.169 | 0.201 | 0.090 | 0.165 |
| Inverse Sqrt. | 0.561 | 0.322 | 0.456 | 0.219 | 0.097 | 0.180 | 0.196 | 0.068 | 0.166 | 0.198 | 0.077 | 0.161 |
| Piecewise | 0.649 | 0.407 | 0.477 | 0.245 | 0.144 | 0.197 | 0.197 | 0.087 | 0.170 | 0.204 | 0.096 | 0.166 |

4.3 Ablation Studies

Score-to-Weight Function. In this study, we examine the effectiveness of various score-to-weight (STW) functions on various metrics in Table 3. We evaluate five distinct STW functions: Constant, Linear, Inverse, Inverse Square Root, and Piecewise. The Constant function serves as our baseline, reflecting the unweighted loss approach common in traditional contrastive learning methods [18]. In contrast, the Linear function, which directly applies the ranking scores as weights, demonstrated notable enhancements over the baseline in all tested scenarios, underscoring the value of integrating ranking information into the training process. The Inverse function, adjusting weight distribution to prioritize pairs with higher scores, shows improvement across all metrics relative to the Linear approach, particularly in the ERR metric, which primarily evaluates the top relevant document. The performance of inverse function for ERR has gained **591%** for In-domain and **40.0% - 117%** for the other evaluations relative to the baseline, highlighting its strength in prioritizing pairs with top scores. The Inverse Square Root function occupies a middle ground between the Linear and Inverse functions, generally underperforming compared to the Inverse across the evaluated metrics. The Piecewise function is designed to assign equal weights to the top 10% of documents for a given query, aligning well with the NDCG@10 metric. Consequently, it has achieved significant improvements in NDCG@10, showing a **54.9%** increase for In-domain and **2.6%-24.4%** for other settings relative to the baseline. For other metrics, its performance is comparable to that of the Inverse function. This illustrates how GCL can be tailored to focus on different metrics in a commercial setting. For the other experiments in this paper, we employ the Inverse function as it is natural and consistently performs well.

Multi-Field weight γ_{R_1} for document. In this analysis, we use product image and title as RHS fields to represent the document. In calculating \mathbf{Z}_{avg} , discussed in Section 3.4, we assign weight γ_{R_1} to the image field and γ_{R_2} to the title field, with $\gamma_{R_2} = 1 - \gamma_{R_1}$. In this study, we experimented with varying γ_{R_1} values of 1, 0.9, 0.5, 0.1, and 0, where a value of 1 represents purely image embedding, 0 corresponds to purely title embedding, and the intermediate values signify weighted averages between image and title embeddings. We conduct this ablation study with the GSFashion-5M dataset, roughly half of the full dataset, to accelerate experimentation. The result in Table 2 shows that the model performs the best

Table 3: Performance comparison of GCL multi-field with varying image weight γ_{R_1} using the GSFashion-5M dataset and ViTB32 [30] model. The last row represents the setting where γ_{R_1} equals 0.5 for in-domain and 0 for all other evaluations.

| γ_{R_1} | In-Domain | | | Novel Queries | | | Novel Corpus | | | Zero-Shot | | |
|----------------|--------------|--------------|--------------|---------------|--------------|--------------|--------------|--------------|--------------|--------------|--------------|--------------|
| | nDCG | ERR | RBP | nDCG | ERR | RBP | nDCG | ERR | RBP | nDCG | ERR | RBP |
| 1.0 | 0.494 | 0.591 | 0.364 | 0.122 | 0.099 | 0.098 | 0.068 | 0.037 | 0.057 | 0.068 | 0.037 | 0.057 |
| 0.9 | 0.488 | 0.579 | 0.358 | 0.151 | 0.120 | 0.120 | 0.117 | 0.055 | 0.097 | 0.100 | 0.048 | 0.082 |
| 0.5 | 0.599 | 0.608 | 0.459 | 0.236 | 0.141 | 0.190 | 0.197 | 0.084 | 0.169 | 0.201 | 0.090 | 0.165 |
| 0.1 | 0.488 | 0.490 | 0.387 | 0.254 | 0.135 | 0.207 | 0.229 | 0.097 | 0.193 | 0.225 | 0.100 | 0.186 |
| 0.0 | 0.473 | 0.483 | 0.379 | 0.257 | 0.137 | 0.209 | 0.236 | 0.099 | 0.197 | 0.229 | 0.098 | 0.188 |
| 0.5/0.0 | 0.599 | 0.608 | 0.459 | 0.246 | 0.127 | 0.200 | 0.230 | 0.091 | 0.192 | 0.223 | 0.094 | 0.183 |

in in-domain evaluation with γ_{R_1} equals to 0.5, signifying an even 50/50 image and title contribution to the average embedding. Conversely, for cold-start evaluations, the model exhibits optimal results when relying solely on the title field. The integration of pairwise loss between each field on the LHS and each field on the RHS enables the effective use of pure title data, even though the image data is also trained as part of the RHS fields. Consequently, we conducted additional evaluations setting γ_{R_1} to 0.5 for in-domain evaluation and to 0 for various cold-start evaluations, yielding the most favorable outcomes overall. We thus use the 0.5/0.0 setting for the following batch size ablation study in as well as the multi-field experiment in Table 1.

Influence of batch size. Batch size significantly impacts contrastive learning, where larger sizes capture more hard negatives but may also increase false negatives, leading to worse test results. According to Table 4, the performance of ViTB32’s [30] improves incrementally with batch size. The gain starts to diminish from 16k to 24k. For ViTL14 [30], performance decreases starting at a 6k batch size in novel queries evaluation while still improves in other evaluations. Interestingly, despite requiring significantly less computation, ViTB32 matches the performance of ViTL14 in most fields when using large batch sizes. Its ERR performance even surpasses ViTL14 for in-domain and novel queries evaluations.

Table 4: Comparing GCL finetuning with different batch sizes same epochs using ViTB32 [30] and ViTL14 [30] with GSFull-10M dataset.

| | Batch Size | In-Domain | | | Novel Queries | | | Novel Corpus | | | Zero-Shot | | |
|-------------|------------|--------------|--------------|--------------|---------------|--------------|--------------|--------------|--------------|--------------|--------------|--------------|--------------|
| | | nDCG | ERR | RBP | nDCG | ERR | RBP | nDCG | ERR | RBP | nDCG | ERR | RBP |
| ViTB32 [30] | 1024 | 0.516 | 0.486 | 0.401 | 0.271 | 0.135 | 0.224 | 0.265 | 0.107 | 0.223 | 0.245 | 0.102 | 0.204 |
| | 2048 | 0.577 | 0.554 | 0.446 | 0.287 | 0.144 | 0.237 | 0.276 | 0.110 | 0.231 | 0.257 | 0.108 | 0.213 |
| | 4096 | 0.628 | 0.602 | 0.484 | 0.297 | 0.152 | 0.243 | 0.283 | 0.111 | 0.236 | 0.264 | 0.110 | 0.217 |
| | 8192 | 0.663 | 0.640 | 0.509 | 0.306 | 0.157 | 0.249 | 0.288 | 0.111 | 0.239 | 0.268 | 0.110 | 0.220 |
| | 16324 | 0.683 | 0.666 | 0.519 | 0.310 | 0.165 | 0.251 | 0.292 | 0.112 | 0.241 | 0.269 | 0.113 | 0.204 |
| | 24576 | 0.683 | 0.689 | 0.515 | 0.313 | 0.171 | 0.252 | 0.292 | 0.117 | 0.241 | 0.270 | 0.113 | 0.204 |
| ViTL14 | 2048 | 0.603 | 0.562 | 0.467 | 0.305 | 0.156 | 0.251 | 0.288 | 0.118 | 0.241 | 0.272 | 0.114 | 0.224 |
| | 4096 | 0.663 | 0.610 | 0.514 | 0.318 | 0.163 | 0.259 | 0.294 | 0.118 | 0.244 | 0.274 | 0.114 | 0.226 |
| | 6144 | 0.690 | 0.630 | 0.535 | 0.274 | 0.114 | 0.226 | 0.320 | 0.164 | 0.261 | 0.293 | 0.115 | 0.244 |

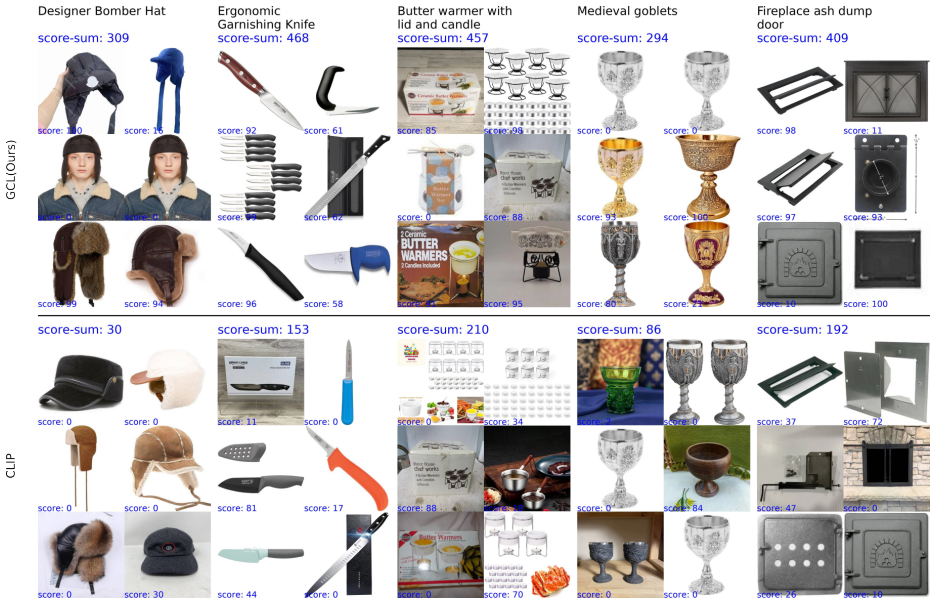


Fig. 4: Visualization of the retrieval performance of ViTL14 trained by GCL(ours) and CLIP [30]. Five queries are shown in the top, and the top-6 retrieved items are demonstrated. Score-sum represents the total ground-truth scores of the six items.

4.4 Qualitative Results

In the visual analysis illustrated in Figure 4, we compare the top-6 products retrieved by ViTL14 [30] models fine-tuned with both GCL and CLIP [30] for five randomly selected queries from the in-domain set. While the products retrieved by both methods seem visually relevant to the queries, the GCL-trained model excels at ranking products with higher ground truth scores at the top. This discrepancy creates a substantial gap in the cumulative ground-truth ranking scores between the two approaches. GCL outperforms its baseline in scenarios where document ranking is critical.

5 Conclusion

In this work, we show that the current contrastive learning approaches fail to incorporate direct ranking signal leading to low retrieval performance. To address the gap, we first acquire a large-scale dataset with fine-grained relevance scores to support the research community. Following that, we propose GCL, which integrates nuanced ranking information and train with multi-field query and document. GCL has surpassed conventional methods by a large margin. Its effectiveness will unlock numerous practical applications including vector search. Future improvements can be made by improving the multi-field with a learnable late interaction module, adapting to in-domain and cold-start scenarios.

References

1. Achiam, J., Adler, S., Agarwal, S., Ahmad, L., Akkaya, I., Aleman, F.L., Almeida, D., Altenschmidt, J., Altman, S., Anadkat, S., et al.: Gpt-4 technical report. arXiv preprint arXiv:2303.08774 (2023) [5](#)
2. Bonifacio, L., Abonizio, H., Fadaee, M., Nogueira, R.: Inpars: Data augmentation for information retrieval using large language models. arXiv preprint arXiv:2202.05144 (2022) [4](#)
3. Boteva, V., Gholipour, D., Sokolov, A., Riezler, S.: A full-text learning to rank dataset for medical information retrieval. In: Advances in Information Retrieval: 38th European Conference on IR Research, ECIR 2016, Padua, Italy, March 20–23, 2016. Proceedings 38. pp. 716–722. Springer (2016) [5](#)
4. Chapelle, O., Metzler, D., Zhang, Y., Grinspan, P.: Expected reciprocal rank for graded relevance. In: Proceedings of the 18th ACM Conference on Information and Knowledge Management. p. 621–630. CIKM '09, Association for Computing Machinery, New York, NY, USA (2009). <https://doi.org/10.1145/1645953.1646033>, <https://doi.org/10.1145/1645953.1646033> [10](#)
5. Cherti, M., Beaumont, R., Wightman, R., Wortsman, M., Ilharco, G., Gordon, C., Schuhmann, C., Schmidt, L., Jitsev, J.: Reproducible scaling laws for contrastive language-image learning. In: Proceedings of the IEEE/CVF Conference on Computer Vision and Pattern Recognition (CVPR). pp. 2818–2829 (June 2023) [2](#), [9](#), [11](#), [19](#)
6. Craswell, N., Mitra, B., Yilmaz, E., Campos, D., Voorhees, E.M.: Overview of the trec 2019 deep learning track. arXiv preprint arXiv:2003.07820 (2020) [1](#), [3](#)
7. Frej, J., Mulhem, P., Schwab, D., Chevallet, J.P.: Learning term discrimination. In: Proceedings of the 43rd International ACM SIGIR Conference on Research and Development in Information Retrieval. p. 1993–1996. SIGIR '20, Association for Computing Machinery, New York, NY, USA (2020). <https://doi.org/10.1145/3397271.3401211>, <https://doi.org/10.1145/3397271.3401211> [4](#)
8. Gutmann, M., Hyvärinen, A.: Noise-contrastive estimation: A new estimation principle for unnormalized statistical models. In: Teh, Y.W., Titterton, M. (eds.) Proceedings of the Thirteenth International Conference on Artificial Intelligence and Statistics. Proceedings of Machine Learning Research, vol. 9, pp. 297–304. PMLR, Chia Laguna Resort, Sardinia, Italy (13–15 May 2010), <https://proceedings.mlr.press/v9/gutmann10a.html> [1](#)
9. Jaiswal, A., Babu, A.R., Zadeh, M.Z., Banerjee, D., Makedon, F.: A survey on contrastive self-supervised learning. Technologies **9**(1) (2021). <https://doi.org/10.3390/technologies9010002>, <https://www.mdpi.com/2227-7080/9/1/2> [1](#)
10. Jang, K.R., Kang, J., Hong, G., Myaeng, S.H., Park, J., Yoon, T., Seo, H.: Ultra-high dimensional sparse representations with binarization for efficient text retrieval. arXiv preprint arXiv:2104.07198 (2021) [4](#)
11. Järvelin, K., Kekäläinen, J.: Cumulated gain-based evaluation of ir techniques. ACM Trans. Inf. Syst. **20**(4), 422–446 (oct 2002). <https://doi.org/10.1145/582415.582418>, <https://doi.org/10.1145/582415.582418> [9](#)
12. Jeronimo, V., Bonifacio, L., Abonizio, H., Fadaee, M., Lotufo, R., Zavrel, J., Nogueira, R.: Inpars-v2: Large language models as efficient dataset generators for information retrieval. arXiv preprint arXiv:2301.01820 (2023) [4](#)
13. Jia, C., Yang, Y., Xia, Y., Chen, Y.T., Parekh, Z., Pham, H., Le, Q., Sung, Y.H., Li, Z., Duerig, T.: Scaling up visual and vision-language representation

- learning with noisy text supervision. In: Meila, M., Zhang, T. (eds.) Proceedings of the 38th International Conference on Machine Learning. Proceedings of Machine Learning Research, vol. 139, pp. 4904–4916. PMLR (18–24 Jul 2021), <https://proceedings.mlr.press/v139/jia21b.html> 1, 2, 7, 8
14. Kenton, J.D.M.W.C., Toutanova, L.K.: Bert: Pre-training of deep bidirectional transformers for language understanding. In: Proceedings of naacL-HLT. vol. 1, p. 2 (2019) 4
 15. Khattab, O., Zaharia, M.: Colbert: Efficient and effective passage search via contextualized late interaction over bert. In: Proceedings of the 43rd International ACM SIGIR Conference on Research and Development in Information Retrieval. p. 39–48. SIGIR '20, Association for Computing Machinery, New York, NY, USA (2020). <https://doi.org/10.1145/3397271.3401075>, <https://doi.org/10.1145/3397271.3401075> 4
 16. Kwiatkowski, T., Palomaki, J., Redfield, O., Collins, M., Parikh, A., Alberti, C., Epstein, D., Polosukhin, I., Devlin, J., Lee, K., et al.: Natural questions: a benchmark for question answering research. Transactions of the Association for Computational Linguistics 7, 453–466 (2019) 1, 3
 17. Lassance, C., Formal, T., Clinchant, S.: Composite code sparse autoencoders for first stage retrieval. In: Proceedings of the 44th International ACM SIGIR Conference on Research and Development in Information Retrieval. p. 2136–2140. SIGIR '21, Association for Computing Machinery, New York, NY, USA (2021). <https://doi.org/10.1145/3404835.3463066>, <https://doi.org/10.1145/3404835.3463066> 4
 18. Li, M., Liu, X., van de Weijer, J., Raducanu, B.: Learning to rank for active learning: A listwise approach. In: 2020 25th International Conference on Pattern Recognition (ICPR). pp. 5587–5594 (2021). <https://doi.org/10.1109/ICPR48806.2021.9412680> 11, 12
 19. Liu, Y., Ott, M., Goyal, N., Du, J., Joshi, M., Chen, D., Levy, O., Lewis, M., Zettlemoyer, L., Stoyanov, V.: Roberta: A robustly optimized bert pretraining approach. arXiv preprint arXiv:1907.11692 (2019) 10, 11, 19
 20. Luo, H., Ji, L., Zhong, M., Chen, Y., Lei, W., Duan, N., Li, T.: Clip4clip: An empirical study of clip for end to end video clip retrieval and captioning. Neurocomputing 508, 293–304 (2022). <https://doi.org/https://doi.org/10.1016/j.neucom.2022.07.028>, <https://www.sciencedirect.com/science/article/pii/S0925231222008876> 1, 2
 21. Ma, H., Zhao, H., Lin, Z., Kale, A., Wang, Z., Yu, T., Gu, J., Choudhary, S., Xie, X.: Ei-clip: Entity-aware interventional contrastive learning for e-commerce cross-modal retrieval. In: Proceedings of the IEEE/CVF Conference on Computer Vision and Pattern Recognition (CVPR). pp. 18051–18061 (June 2022) 1, 2
 22. Mackenzie, J., Dai, Z., Gallagher, L., Callan, J.: Efficiency implications of term weighting for passage retrieval. In: Proceedings of the 43rd International ACM SIGIR Conference on Research and Development in Information Retrieval. p. 1821–1824. SIGIR '20, Association for Computing Machinery, New York, NY, USA (2020). <https://doi.org/10.1145/3397271.3401263>, <https://doi.org/10.1145/3397271.3401263> 4
 23. Maia, M., Handschuh, S., Freitas, A., Davis, B., McDermott, R., Zarrouk, M., Balahur, A.: Www'18 open challenge: financial opinion mining and question answering. In: Companion proceedings of the the web conference 2018. pp. 1941–1942 (2018) 1, 3

24. Moffat, A., Zobel, J.: Rank-biased precision for measurement of retrieval effectiveness. *ACM Trans. Inf. Syst.* **27**(1) (dec 2008). <https://doi.org/10.1145/1416950.1416952>, <https://doi.org/10.1145/1416950.1416952> 10
25. Mokady, R., Hertz, A., Bermano, A.H.: Clipcap: Clip prefix for image captioning. arXiv preprint arXiv:2111.09734 (2021) 2
26. Nguyen, T., Rosenberg, M., Song, X., Gao, J., Tiwary, S., Majumder, R., Deng, L.: Ms marco: A human generated machine reading comprehension dataset. *choice* **2640**, 660 (2016) 1, 3, 5
27. Nie, P., Zhang, Y., Geng, X., Ramamurthy, A., Song, L., Jiang, D.: Dc-bert: Decoupling question and document for efficient contextual encoding. In: Proceedings of the 43rd International ACM SIGIR Conference on Research and Development in Information Retrieval. p. 1829–1832. SIGIR '20, Association for Computing Machinery, New York, NY, USA (2020). <https://doi.org/10.1145/3397271.3401271>, <https://doi.org/10.1145/3397271.3401271> 4
28. Nogueira, R., Yang, W., Lin, J., Cho, K.: Document expansion by query prediction. arXiv preprint arXiv:1904.08375 (2019) 4
29. Oord, A.v.d., Li, Y., Vinyals, O.: Representation learning with contrastive predictive coding. arXiv preprint arXiv:1807.03748 (2018) 1, 2, 8
30. Radford, A., Kim, J.W., Hallacy, C., Ramesh, A., Goh, G., Agarwal, S., Sastry, G., Askell, A., Mishkin, P., Clark, J., Krueger, G., Sutskever, I.: Learning transferable visual models from natural language supervision. In: Meila, M., Zhang, T. (eds.) Proceedings of the 38th International Conference on Machine Learning. Proceedings of Machine Learning Research, vol. 139, pp. 8748–8763. PMLR (18–24 Jul 2021), <https://proceedings.mlr.press/v139/radford21a.html> 1, 2, 6, 7, 8, 9, 11, 12, 13, 14, 19, 20
31. Robertson, S.E., Walker, S., Jones, S., Hancock-Beaulieu, M.M., Gatford, M., et al.: Okapi at trec-3. *Nist Special Publication Sp* **109**, 109 (1995) 10, 11
32. Santhanam, K., Khattab, O., Saad-Falcon, J., Potts, C., Zaharia, M.: Colbertv2: Effective and efficient retrieval via lightweight late interaction. arXiv preprint arXiv:2112.01488 (2021) 4
33. Schroff, F., Kalenichenko, D., Philbin, J.: Facenet: A unified embedding for face recognition and clustering. In: Proceedings of the IEEE Conference on Computer Vision and Pattern Recognition (CVPR) (June 2015) 1
34. Soboroff, I., Huang, S., Harman, D.: Trec 2018 news track overview. In: TREC. vol. 409, p. 410 (2018) 5
35. Sohn, K.: Improved deep metric learning with multi-class n-pair loss objective. In: Lee, D., Sugiyama, M., Luxburg, U., Guyon, I., Garnett, R. (eds.) Advances in Neural Information Processing Systems. vol. 29. Curran Associates, Inc. (2016), https://proceedings.neurips.cc/paper_files/paper/2016/file/6b180037abbeba991d8b1232f8a8ca9-Paper.pdf 1
36. Suarez, A., Albakour, D., Corney, D., Martinez, M., Esquivel, J.: A data collection for evaluating the retrieval of related tweets to news articles. In: Advances in Information Retrieval: 40th European Conference on IR Research, ECIR 2018, Grenoble, France, March 26–29, 2018, Proceedings 40. pp. 780–786. Springer (2018) 1, 3
37. Thakur, N., Reimers, N., Rücklé, A., Srivastava, A., Gurevych, I.: Beir: A heterogeneous benchmark for zero-shot evaluation of information retrieval models. arXiv preprint arXiv:2104.08663 (2021) 1, 5
38. Tsatsaronis, G., Balikas, G., Malakasiotis, P., Partalas, I., Zschunke, M., Alvers, M.R., Weissenborn, D., Krithara, A., Petridis, S., Polychronopoulos, D., et al.:

- An overview of the biosq large-scale biomedical semantic indexing and question answering competition. *BMC bioinformatics* **16**(1), 1–28 (2015) **3**
39. Vasu, P.K.A., Pouransari, H., Faghri, F., Vemulapalli, R., Tuzel, O.: Mobileclip: Fast image-text models through multi-modal reinforced training. arXiv preprint arXiv:2311.17049 (2023) **2**
 40. Vedit, V., Engilberge, M., Salzmann, M.: Clip the gap: A single domain generalization approach for object detection. In: Proceedings of the IEEE/CVF Conference on Computer Vision and Pattern Recognition (CVPR). pp. 3219–3229 (June 2023) **2**
 41. Voorhees, E., Alam, T., Bedrick, S., Demner-Fushman, D., Hersh, W.R., Lo, K., Roberts, K., Soboroff, I., Wang, L.L.: Trec-covid: constructing a pandemic information retrieval test collection. In: ACM SIGIR Forum. vol. 54, pp. 1–12. ACM New York, NY, USA (2021) **1, 3**
 42. Wadden, D., Lin, S., Lo, K., Wang, L.L., van Zuylen, M., Cohan, A., Hajishirzi, H.: Fact or fiction: Verifying scientific claims. arXiv preprint arXiv:2004.14974 (2020) **3, 5**
 43. Wang, L., Yang, N., Huang, X., Jiao, B., Yang, L., Jiang, D., Majumder, R., Wei, F.: Text embeddings by weakly-supervised contrastive pre-training. arXiv preprint arXiv:2212.03533 (2022) **10, 11, 19**
 44. Yan, M., Li, C., Bi, B., Wang, W., Huang, S.: A unified pretraining framework for passage ranking and expansion. Proceedings of the AAAI Conference on Artificial Intelligence **35**(5), 4555–4563 (May 2021). <https://doi.org/10.1609/aaai.v35i5.16584>, <https://ojs.aaai.org/index.php/AAAI/article/view/16584> **4**
 45. Yang, Z., Qi, P., Zhang, S., Bengio, Y., Cohen, W.W., Salakhutdinov, R., Manning, C.D.: Hotpotqa: A dataset for diverse, explainable multi-hop question answering. arXiv preprint arXiv:1809.09600 (2018) **1, 3**
 46. Yu, H., Xiong, C., Callan, J.: Improving query representations for dense retrieval with pseudo relevance feedback. In: Proceedings of the 30th ACM International Conference on Information & Knowledge Management. p. 3592–3596. CIKM '21, Association for Computing Machinery, New York, NY, USA (2021). <https://doi.org/10.1145/3459637.3482124>, <https://doi.org/10.1145/3459637.3482124> **4**
 47. Yu, J., Wang, Z., Vasudevan, V., Yeung, L., Seyedhosseini, M., Wu, Y.: Coca: Contrastive captioners are image-text foundation models. arXiv preprint arXiv:2205.01917 (2022) **1, 2, 7, 8**
 48. Yuan, L., Chen, D., Chen, Y.L., Codella, N., Dai, X., Gao, J., Hu, H., Huang, X., Li, B., Li, C., et al.: Florence: A new foundation model for computer vision. arXiv preprint arXiv:2111.11432 (2021) **1, 2**
 49. Zhai, X., Mustafa, B., Kolesnikov, A., Beyer, L.: Sigmoid loss for language image pre-training. arXiv preprint arXiv:2303.15343 (2023) **2, 9, 11, 19**
 50. Zhao, W.X., Liu, J., Ren, R., Wen, J.R.: Dense text retrieval based on pretrained language models: A survey. arXiv preprint arXiv:2211.14876 (2022) **4**
 51. Zhou, K., Yang, J., Loy, C.C., Liu, Z.: Conditional prompt learning for vision-language models. In: Proceedings of the IEEE/CVF Conference on Computer Vision and Pattern Recognition (CVPR). pp. 16816–16825 (June 2022) **2**
 52. Zhou, K., Yang, J., Loy, C.C., Liu, Z.: Learning to prompt for vision-language models. *International Journal of Computer Vision* **130**(9), 2337–2348 (2022) **2**

In the followin Appendices, we start with clarifications regarding the Roberta and Multi-field experiments, followed by a discussion on the weighted sigmoid loss. We then proceed to delve into additional experimental details. Finally, we showcase more visual examples from the proposed GS-Full-10M dataset.

A Clarifications

A.1 Roberta Experiments

In the text-only section of Table 1, we conducted experiments using the Roberta base model [19]. For the pre-trained model, we utilized the version provided by OpenClip [5]. For fine-tuning, we employed a similar contrastive cross-entropy loss as described in [43] and [30], without incorporating reconstruction objectives like next token or masked token prediction from the original paper. In summary, for the Roberta models, it is more accurate to update the "Method" designation from "RoBERTa" to "Contrastive Cross Entropy" for row 4-5.

A.2 Multi-Field Formulation and Experiments

In this paper, we expanded traditional single-field contrastive learning to accommodate multiple fields, utilizing left-hand-side (LHS) and right-hand-side (RHS) fields for the two inputs. Due to limitations in existing datasets, our demonstration focused solely on multi-field documents comprising text titles and image thumbnails. However, given the symmetrical nature of our approach, we anticipate its extension to multi-field queries as well.

B Weighted Sigmoid Loss

Unlike cross-entropy loss, the sigmoid loss operates directly on individual pairs without relying on a normalization process [49]. This implies that the loss calculated for each pair is independent of other pairs in the dataset. The ground truth matrix is 1 in the diagonal and -1 one everywhere else. To incorporate ranking signals, we simply multiply this diagonal with weights. The loss is calculated as,

$$\mathcal{L}_{WSIG}(\mathbf{Z}, \mathbf{w}) = -\frac{1}{N} \sum_{i=1}^N \sum_{j=1}^N \log \frac{1}{1 + \exp(W[i, j](-t\mathbf{Z}[i, j] + b))} \quad (6)$$

where t and b are learnable logit scale and bias. The weight matrix $W \in \mathbb{R}^{N \times N}$ is constructed such that its diagonal entries are equal to the weights \mathbf{w} , and all off-diagonal values are set to -1. The weighted sigmoid loss offers the advantage of decoupling the loss calculation for individual pairs from the batch context, albeit at the cost of requiring more hyper-parameter (logit scale and bias) tuning and taking longer to converge.

Results. As a baseline, we trained a ViT-B/16 model [30] using the original SigLip sigmoid loss on the GS-Full-10M dataset. Subsequently, we trained another ViT-B/16 [30] using our GCL framework under identical dataset conditions and hyperparameters. The outcomes of both models are presented in Table 1 image-only section. Model trained with GCL weighted sigmoid loss outperforms the baseline by a large margin. On the other hand, for in-domain evaluation, both the baseline and the GCL-enhanced model significantly underperform two

VITB32 models trained with cross entropy and weighted cross entropy losses, respectively, despite VITB32 being smaller than VITB16. They perform on par for the cold-start evaluations. We believe that the observed performance discrepancy might be due to sigmoid losses take longer to converge compared to cross entropy losses.

C Additional experimental Details

We also examined the impact of weight decay parameters 0.02 and 0.00001 on the VITB32 model. The outcomes, presented in Table A, show negligible differences between the two significantly varying weight decay values.

Table A: Comparing GCL finetuning with different weight decay values with same epochs using ViTB32 [30] with GSFull-10M dataset.

| Weight Decay | In-Domain | | | Novel Queries | | | Novel Corpus | | | Zero-Shot | | |
|--------------|-----------|-------|-------|---------------|-------|-------|--------------|-------|-------|-----------|-------|-------|
| | nDCG | ERR | RBP | nDCG | ERR | RBP | nDCG | ERR | RBP | nDCG | ERR | RBP |
| 0.02 | 0.663 | 0.640 | 0.509 | 0.306 | 0.157 | 0.249 | 0.288 | 0.111 | 0.239 | 0.268 | 0.110 | 0.220 |
| 0.00001 | 0.663 | 0.637 | 0.509 | 0.307 | 0.157 | 0.250 | 0.287 | 0.111 | 0.238 | 0.268 | 0.110 | 0.220 |

D More dataset Visualization

In the supplementary material, additional visualizations of the GS-Full-10M dataset are presented in Figure A and Figure B. The dataset is displayed in a triplet format, featuring randomly selected queries in the top row and the top 8 related documents ranked by score below each query. For conciseness, only the thumbnail images of the products are shown, and the product titles are omitted.

Protector Full



Large wooden skirt hanger collection



Boys overall shorts



Women Novelty Socks



Aromatherapy mist maker



Low noise fountain pump



Cotton electric blanket



Pajama sets women



unicorn pajamas girls



Vintage Locket Pendant Necklace



Women's gymnastics leotards with skirts



Rug tape for area rugs



Fig. A: More Dataset Visualizations.

Protector Full



Large wooden skirt hanger collection



Boys overall shorts



Women Novelty Socks



Aromatherapy mist maker



Low noise fountain pump



Cotton electric blanket



Pajama sets women



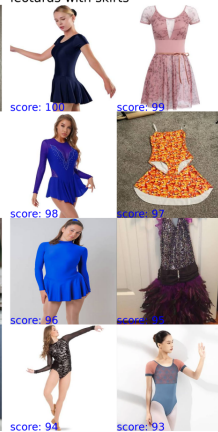
unicorn pajamas girls



Vintage Locket Pendant Necklace



Women's gymnastics leotards with skirts



Rug tape for area rugs



Fig. B: More Dataset Visualizations.